

SPIRAL2 CRYOMODULES: STATUS AND FIRST TESTS RESULTS

G. Olry, D. Longuevergne, H. Sagnac, CNRS/IN2P3, Université Paris-Sud, IPN Orsay, France,
 P. Bosland, CEA Saclay Irfu/SACM,
 Y. Gómez-Martínez, LPSC, UJF, CNRS/IN2P3, INPG. Grenoble, France

Abstract

The SPIRAL2 superconducting linac will be composed of 19 cryomodules of two different types: 12 low-beta cryomodules (so called A) housing a single Quarter-Wave Resonator (QWR) each (beta 0.07, 88 MHz) followed by 7 high-beta cryomodules (so called B), housing a couple of QWRs each (beta 0.12, 88 MHz).

A prototype of each cryomodule type (called qualifying cryomodule) has been constructed by the industry and successfully tested at 4.5 K and high power ($P_{\max}=10$ kW) in 2009. The results of these qualification tests will be presented as well as the status on cryostats, cavities and RF couplers production.

INTRODUCTION

The GANIL's SPIRAL 2 project [1] aims at delivering high intensities of rare isotope beams by adopting the best production method for each respective radioactive beam. The unstable beams will be produced by the ISOL "Isotope Separation On-Line" method via a converter, or by direct irradiation of fissile material. On the basis of referee reports of international experts and committees, the positive evaluations by IN2P3/CNRS and DSM/CEA, GANIL, and the support of the region of Basse-Normandie, the French Minister of Research took the decision on the construction of SPIRAL 2 in May 2005.

The driver will accelerate protons (0.15 to 5 mA – 33 MeV), deuterons (0.15 to 5 mA – 40 MeV) and heavy ions (up to 1 mA, Q/A=1/3 14.5 MeV/u to 1/6 8.5 MeV/A). The superconducting linac is composed of a low energy section with 12 cryomodules A with one cavity ($\beta=0.07$) followed by a high energy section composed of 7 cryomodules B housing two cavities ($\beta=0.12$), see Fig. 1. Doublets of warm quadrupoles and diagnostics are inserted between each cryomodule.

Cryomodules A are developed by CEA/Saclay while cryomodules B are developed by IPN/Orsay. Both types of cavities will be equipped with the same power coupler, designed for a maximum power of 40 kW CW (in Travelling Wave mode), developed and conditioned at LPSC Grenoble [2].

General development programs are quite similar for

both cryomodule types: the qualifying cryomodules have been firstly tested at low power (critical coupling with antenna) [3] then at high-power this year before starting the series production. These two qualifying cryomodules will be part of the driver with minor modifications which we will detail hereafter. Cryostats, cavities and power couplers productions have started. Cavities are firstly tested in vertical cryostat then mounted together with a power coupler inside their cryomodule for high power and final cryogenic test. Therefore, each cryomodule will be individually tested and validated before their shipment to GANIL for their installation in the linac tunnel, in 2011. For that purpose, CEA/Saclay and IPN Orsay have developed their own test stand for cryomodule. Laboratories have also the responsibility of: chemical treatments, High Pressure Rinsing and assembly in clean room.

CRYOMODULE A OVERVIEW

Details on cryomodule and cavity designs were described previously in [4].

Each cryomodule A contains only one QWR, $\beta=0.07$, 88.05 MHz. Due to beam dynamic considerations, the cryostat flange-to-flange length was minimized to 610 mm. This could have been realized by developing the cavity tuning system that deforms the cavity, perpendicularly to the beam axis (Fig. 2). The cavity mechanical design was optimized in order to reach a full tuning range of 25 kHz at 4.5 K without plastic deformation of the niobium cavity.

The capacitive power coupler is mounted vertically on one cavity bottom port. The external coupling factor is set to $5.5 \cdot 10^6$ for all cavities A (fixed coupler) in order to deliver a maximum power of 10 kW at the nominal gradient of 6.5 MV/m (accelerating length defined as $\beta\lambda/2$).

The first cavities of the accelerator low beta section will work at low accelerating field ($E_a \approx 0.5$ MV/m) while the last cavities of the section will work at about $E_a = 6.5$ MV/m.

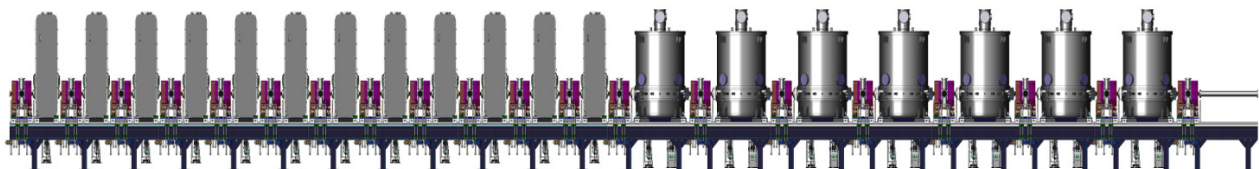


Figure 1: Layout of the linac (total length 35 m).

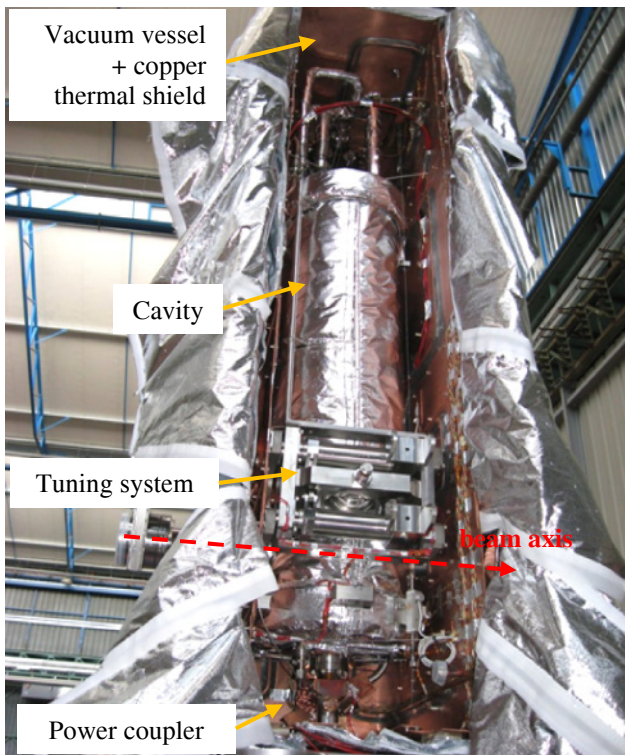


Figure 2: Cryomodule A final preparation before closing.

TEST OF THE CRYOMODULE A

A specific test stand (Fig. 3) has been installed at Saclay in order to qualify all cryomodules A. The 10-kW solid-state amplifier, providing RF power to the cavity, and the cryogenic valves box used for this test, will also be installed in the Linac tunnel.

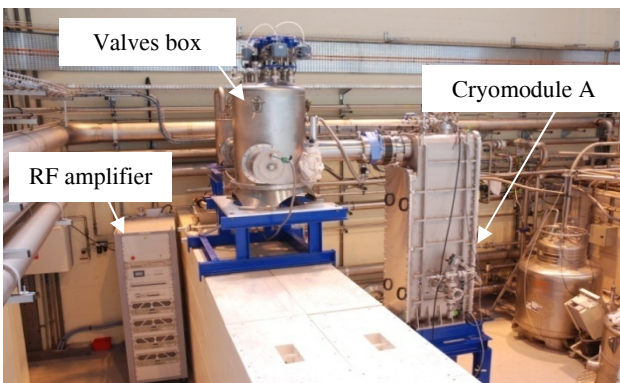


Figure 3: Cryomodule A connected to the valves box and the 10-kW RF amplifier coupler.

The cryomodule was tested with the qualifying cavity (so-called AZ1) that showed abnormal RF dissipations during vertical cryostat tests ($Q_0=2 \cdot 10^8$ instead of expected $2 \cdot 10^9$). The assembly of the cryomodule with this cavity was made before we found the reasons of those losses [5]. In this configuration, the cavity dissipation was 100 W at its maximum accelerating field ($E_a=11$ MV/m), leading us to modify the cryogenic system, initially designed for a 40 W maximum load.

08 Ancillary systems

RF power tests were performed from end of December 2008 to April 2009. As the large clean room that is being built at Saclay was not ready at that time, all the cryomodule assembly has been performed in the IPN Orsay SUPRATEch clean room. This operation was made by CEA Saclay's team with the help of the cryomodule B team of IPN Orsay.

Cryogenic Measurements

The copper thermal shield is cooled down first to about 100 K. Before the cavity temperature reaches 250 K, the liquid helium valve is opened and the cavity temperature dropped down to 4.5 K within about 1 hour (see dark blue, curve on Fig. 4). One can note that the tuning system temperature goes down very slowly (> 3 days to reach 50K). The coupler window temperature is regulated around 273°C by mean of "warm" air forced flux (pink curve).

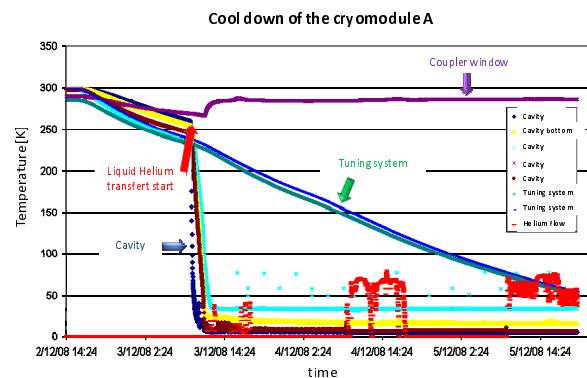


Figure 4: Cool down of the cryomodule A.

Static losses of the cryomodule have been measured by isolating it from the valves box and connecting the helium return gas to a pressure stabilized helium pipe. The measurement of the return gas flow and of the helium level decrease gave us the same result: between 6.5 W and 7.0 W. These values are higher than the theoretical calculations (4 W) but still remain below the SPIRAL2 cryogenic requirement of 8.5 W.

Dynamic cryogenic losses (including the LHe transfer line losses, the valves box losses and the static losses of the cryomodule) have been measured around 35 W. This is higher than expected (about 15 W). One of the reasons was the undersized helium gas return pipe that causes pressure increase, then additional loads. As a consequence, the helium level was difficult to stabilize and modifications of the gas return pipe solve this problem.

Cavity Cool Down

The dismountable Niobium bottom flange of the cavity was thermalized by several copper breads connected to the liquid helium bath. This thermalization was not effective enough, and then the bottom flange temperature remained between 14 K and 17 K (yellow curve on Fig. 4). Taking into account the power coupler load by conduction (1.5 W), further thermal simulations showed

that the copper breads cannot evacuate the load coming through the coupler. The efficiency of this cooling system is in fact limited by the thermal resistance of the contacts between the breads and the copper blocks fixed on the Helium vessel.

RF Power Tests

The power coupler was conditioned up a couple of time to the full power of 10 kW: at room temperature before cooling down and when the cavity was at 4.5 K. Conditioning was performed at 89 MHz, 90 MHz and 87.69 MHz (i.e. the cavity frequency at 300K) at 50 Hz repetition rate and impulsion width ranging from 20 μ s to CW. Multipactor barriers appeared during conditioning at 300 K at 4, 26, 131 and 220 W. Those barriers systematically reappeared after conditioning of the next level.

External Q factor has been measured by two means transmission method: using the 10-kW amplifier and a network analyser, and using the decay time factor (at low field, 5 Hz, 5% duty cycle). Measured values are $5.2 \cdot 10^5$ and $5.4 \cdot 10^5$ respectively, for 7 mm of penetration of the coupler's antenna inside the cavity. This is in very good agreement with calculations: $5.5 \cdot 10^5$

The RF power test was hampered by the low Q factor of the AZ1 cavity. The RF losses of the cavity were about 10 times higher than expected, thus the RF power dissipated by the cavity was about 35 W at 6.5 MV/m accelerating field (i.e. the design accelerating gradient).

The maximum accelerating field reached was 10.3 MV/m, above the design value required by the SPIRAL 2 project (6.5 MV/m). However, the duty cycle was reduced down to 5% (5 Hz) in order to limit the thermal load that could make the cryogenic system unstable.

Continuous mode could be maintained at 6.5 MV/m for about 40 minutes.

Tests of the Tuning System

As described in previous papers, the tuning system works by deforming the cavity in the region of the accelerating gaps [6]. The tuning system is screwed on the cavity on one side, and a sliding system was put on the other side. Therefore, it can be used to squeeze the cavity but not to pull it. The cavity has to be tuned in such a way that at the working frequency (88.052 MHz at 4.5 K) the tuner is working around the middle of its full tuning range (25 kHz).

For the first test, the tuning system was initially just on contact with the cavity (at the extremity of its stroke), and not bolted to it. After a first cooling down and warming up cycle, the cavity frequency was permanently lowered by 5 kHz. This can be explained by the differential shrinkage between niobium (of the cavity) and stainless steel (of the tuning system) (see Fig. 5).

During the cool down of the copper thermal shield with nitrogen (0 to 1500 min on Fig. 5), the cavity and the tuning system temperatures were decreasing slowly. As the tuning system, made of stainless steel, shrinks three

times more than the niobium cavity, the cavity is squeezed by the tuning system.

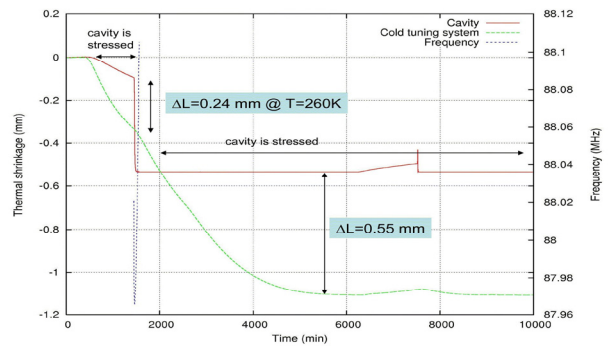


Figure 5: Differential shrinkage of the cavity and tuning system during cool down.

During the cool down with liquid Helium (from 1500 min on Fig. 5), the shrinkage of the cavity is higher than the one of the tuning system: thus, the cavity is free. Then, while the tuning system temperature cools down slowly, its shrinkage becomes once more higher than the one of the cavity, now stabilized at 4.5 K (between 2000 and 6000 min on Fig. 5). As a consequence, the cavity is constrained one more time. It shall be remembered that the niobium elastic limit is 40 MPa at room temperature and around 400 MPa at 4 K. Therefore, while the deformations caused by the differential shrinkage at 4.5 K remain only in the elastic domain, the cavity is plastically deformed during the nitrogen cool down phase.

Thus, before any cool down, the tuning system shall be placed some 1.3 mm away from the cavity. This was performed during the next cool downs and no more permanent frequency shifts were observed.

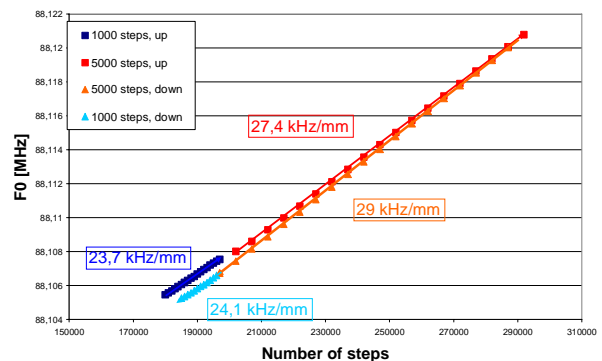


Figure 6: Cavity frequency versus the motor steps (the slight hysteresis of 1 kHz disappeared after 2 cycles).

The measured sensitivity of the tuning system is about 27 kHz/mm (25 kHz/mm expected). Full excursion of the tuning system and way back show a slight hysteresis of about 1 kHz (Fig. 6). This hysteresis disappeared after 2 cycles. Frequency linearity downward is slightly better than upward. One can explain it by the fact that the tuner contact on the cavity is better when the force applied is stronger.

Cavity Alignment

Alignment tolerances of the cavities' beam axis in the SPIRAL 2 superconducting LINAC are ± 1 mm.

Displacements of the cavity inside the cryomodule during pumping, cool down and warming up operations have been measured by two means. First, the beam port flanges of the cavity were equipped with special copper vacuum seals. These seals were machined with lug-shaped sights (three per seal), which allowed to check the cavity movements by optical means in all directions. Second, a displacement sensor (Swema) qualified for cryogenic temperatures operation was mounted on the bottom flange of the cavity. The movable part of the captor was tied on the cryostat top and bottom walls with an Invar wire in order to check vertical displacement of the cavity.

Pumping shows a vertical displacement of the beam axis lower than 0.1 mm.

Cool down show a vertical displacement of 1.13 mm by optical method and 1.07 mm by the displacement captor. No horizontal displacement is measured. These measurements are similar to the estimated value of 1.11 mm upward during cool down.

Therefore the cavities will be shifted downward of 1.1 mm during the cryomodule assembly phase in order to compensate for the beam axis displacement during cool down.

CRYOMODULES AND CAVITIES A PRODUCTION STATUS

Cryomodules

The production of 11 cryomodules A has started in June 2009. The first cryomodule shall be delivered at the beginning of 2010 and tested for validation. Then, the 10 following ones will be delivered between July and December 2010.

In parallel, the qualifying cryomodule will be assembled again and tested by the end of 2009. The goal is to test the new magnetic shield. It consists in a 1-mm thick foil of Mumetall[®] set on the inner surface of the cryostat (at room temperature).

Cavities

The two first cavities (AZ2 and AS3) reached the required performances in vertical cryostat tests. Production of the 10 remaining cavities was shared between two manufacturers. Next cavities will be delivered between May and July 2010.

CRYOMODULE B OVERVIEW

Each cryomodule B houses two QWR, beta 0.12, 88.05 MHz cooled at 4.5 K with liquid Helium (Fig. 7). The overall flange-to-flange cryomodule length is 1360 mm (for a resonator flange-to-flange length is 450 mm).

The cryomodule vacuum vessel and the 60 K thermal shield are made from 3 different parts in order to facilitate the assembly inside the clean room and to limit the

probability of dust pollution. Due to the small cryostat dimensions and mainly to the very low tuning sensitivity to cavity body mechanical stiffness ratio, an alternative tuning system has been developed. It consists in a high RRR Niobium plunger, cooled at 4.5 K, which is inserted on the top of the resonator (inside the magnetic volume). The static tuning range is + 50 kHz with a dynamic range of ± 4 kHz. The cavity alignment is performed by optical means. Each of the 14 resonators is specified for a maximum dissipation of 10 W at 6.5 MV/m. The 7 cryomodules are specified for static cryogenic losses of 11 W at 4.5 K.

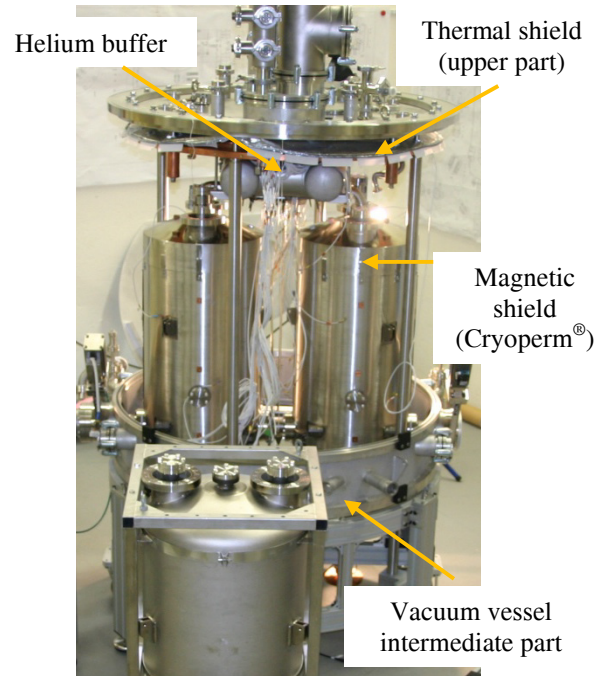


Figure 7: Qualifying cryomodule B

TEST OF THE CRYOMODULE B

The cryomodule B was tested in Orsay in the same conditions as those of the cryomodule A. Each cavity has its own power coupler (two 10 kW amplifiers are installed on site).

Cryogenic Measurements

The thermal shield is cooled by liquid nitrogen at atmospheric pressure (~ 80 K). After 9 hours, the thermal shield is around 80 K and regulated between 80 K and 100 K. The static losses are around 60 W at 80K.

The time needed to cool down the whole helium circuit is estimated at around 5 hours. Both cavities are cooled by the bottom and in parallel through only one feeding valve. The upper parts of cavities and the inner central conductor (stem) remain less than 1 hour between 150 K and 50 K (Fig. 8). This limits significantly possible Q-disease effect.

Once the helium buffer is filled in up to 20%, the liquid helium flows directly into it. An analogical feeding valve controls the helium flow to keep a constant level in the

helium buffer. In this continuous filling mode, the static losses have been measured around 32 W.

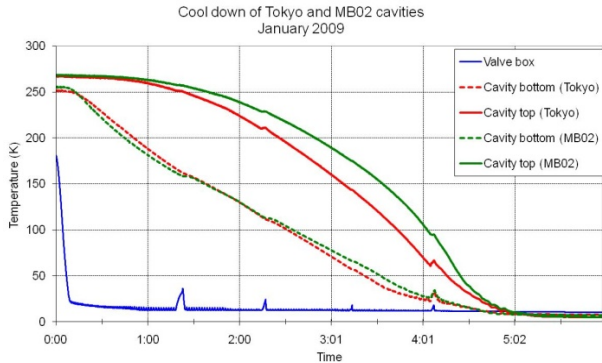


Figure 8: Cavity cool down.

When the feeding valve is closed and the cryomodule is isolated, the static losses fall down to 16 W. Half of losses is due to transfer lines and valves box losses. The theoretical static losses (evaluated at 11 W) are not reached because of undersized heat sinks between the thermal shield and the couplers and the higher temperature of the thermal shield. Measurements at the level of heat sinks have shown that the coupler temperatures stay around 100 K and 120 K.

In continuous filling mode, the helium bath pressure stability is +/- 2 mbar.

Power Coupler Processing

Power couplers have been processed in open loop up to 10 kW in continuous wave. Multipactor barriers and vacuum deteriorations have been recorded only between a few Watts up to 150 W (Fig. 9). It took less than 1 hour to get through. Above 150 W, nothing was observed up to 10 kW. The external coupling factor is equal to 10^6 to achieve a critical coupling at 6.5 MV/m with a 5 mA deuteron beam.

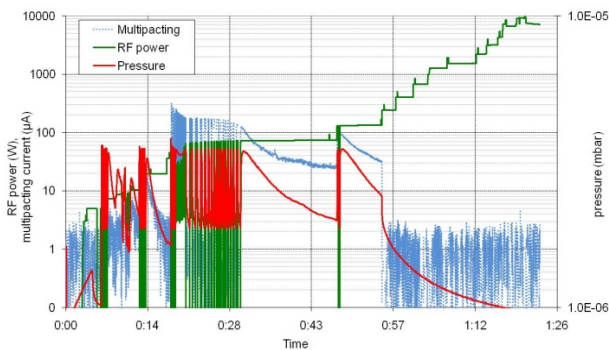


Figure 9: Power coupler conditioning in continuous wave.

RF Power Tests

The unloaded Q_0 has been evaluated through the helium gas flow when all RF power is reflected. At 4.5 K the quality factor at 88 MHz is indeed well above the loaded quality factor. Below 4 MV/m, the RF losses are too small to be accurately measured with respect to the cryogenic static losses. On Fig. 10, we show two different

measurements of Q_0 vs. E_{acc} for the MB02 cavity: in vertical cryostat (critical coupling) and cryomodule (over-coupling). Differences between the two configurations are mainly the tuning system (plunger) and power coupler.

Results in cryomodule are in good agreement with the one in vertical cryostat. The quality factor is not degraded at 6.5 MV/m ($Q_0 > 1.4 \cdot 10^9$), but one can note that the maximal accelerating gradient was lower in the cryomodule configuration (7.2 MV/m instead of 9.2 MV/m in vertical cryostat). We suspect a defect on the plunger of being the cause of that deterioration. This plunger was chemically polished by only several microns.

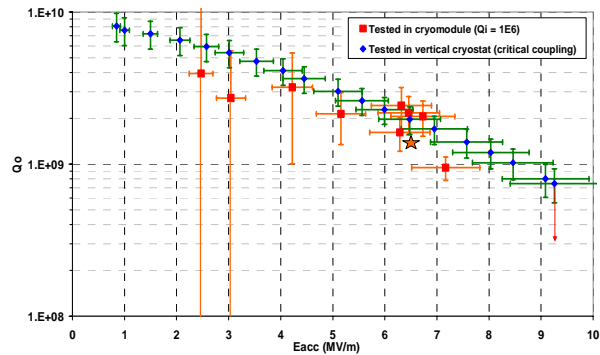


Figure 10: Quality factor versus accelerating gradient in two different configurations for MB02 cavity.

Multipacting, Lorentz Forces Detuning and Pressure Sensitivity

Two multipacting barriers were observed: the first one around 50 kV/m and the second one around 1 MV/m. These barriers were much more easily processed in cryomodule configuration than in vertical cryostat thanks to the power coupler over-coupling.

The frequency shifts during operation are caused by Lorentz forces and pressure drop. The Lorentz factor K has been measured in vertical cryostat where pressure drops are negligible. K was around $-1.8 \text{ Hz}/(\text{MV}/\text{m})^2$. The pressure sensitivity of the cavity has been evaluated to $-7 \text{ Hz}/\text{mbar}$ (same value measured at 300 K).

Test of the Tuning System

Tests on moving plunger have shown an excellent mechanical reliability after hundreds of cycles. The reproducibility of the displacement (stroke of 8 mm) is better than a few microns. The mechanical backlash stays constant around 70 microns over several cycles. This will be compensated, in the case of slow tuning, by implementing in the controller a fast displacement order each time the stepping motor rotation is changing (see example on green curve, Fig. 12).

The tuning sensitivities are linear on the full range and equal to 976 Hz/mm and 908 Hz/mm for diameters of respectively 29.7 mm and 28.5 mm (Fig. 11). These results are in good agreement with simulations. The tuning range is about +/- 4 mm giving a frequency tuning range of about +/- 3.5 kHz. The total reduction of 8

steps/ μm (gear box and ball screw) allows a frequency regulation below 5 Hz or 5° .

We created artificial pressure variations on the Helium bath (by closing the exhaust gases valve) to try to regulate the frequency cavity by the tuning system. The cavity phase and accelerating gradient were regulated by a LLRF loop. The phase error signal consists of the difference between output and input cavity phases. An order, proportional to the phase error was sent each 500 ms to the motor controller. In order to relieve the motor, the order is forced to zero if the phase error is below 5° .

Results are encouraging. Pressure variation up to 32 mbar has been compensated. The phase deviation stays within the cavity bandwidth for pressure perturbations rate lower than 0.4 mbar/s.

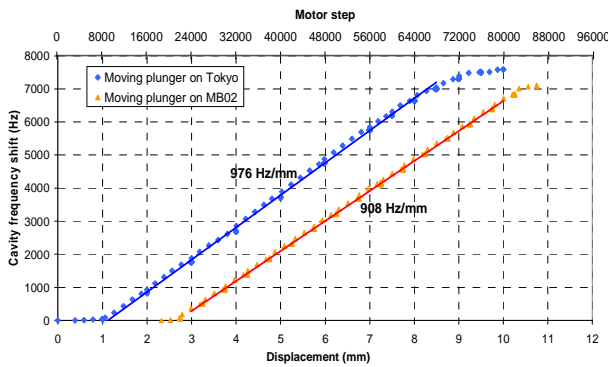


Figure 11: Cavity frequency shift versus displacement for two different plungers.

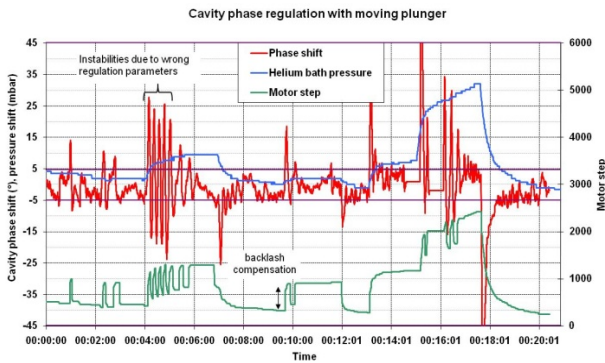


Figure 12: Cavity phase regulation with moving plunger.

CRYOMODULES AND CAVITIES B PRODUCTION

Cryomodules

The production of 6 cryomodules B has started in March 2009. The first cryomodule shall be delivered mid November 2009. After a 2-month test period and its validation, the 5 remaining cryomodules will be delivered every 3 months.

A new intermediate part of the vacuum vessel is delivered end of September 2009 and will replace existing one (shown on Fig. 7). Modifications on flanges will make this qualifying cryomodule be part of the Linac.

08 Ancillary systems

Cavities

Production of the 16 beta 0.12 cavities will end in November 2009. Among about ten cavities already delivered, seven have been already tested and validated at 4.5 K in vertical cryostat (Fig. 13). One is ready for testing and the two others are being BCP treated.

Cavity MB03 has been baked for 55h at 110°C . Losses at 6.5 MV/m have been reduced by 37% ($7\text{ W} \rightarrow 4.4\text{ W}$).

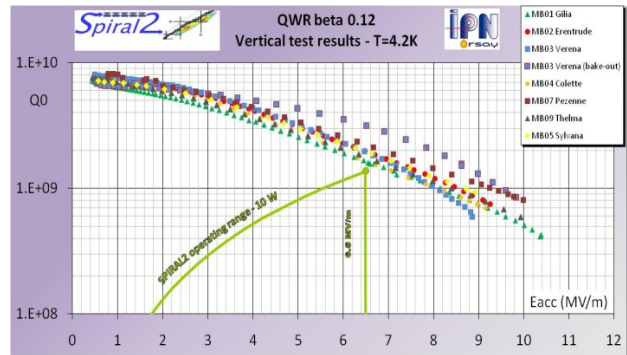


Figure 13: Vertical test results

POWER COUPLERS PRODUCTION AND RF CONDITIONING

The Laboratory of Subatomic Physics and Cosmology (LPSC) in Grenoble has made the design of the power coupler (electromagnetic, thermal and mechanical simulations) and produced the technical drawings for fabrication. They are also in charge of the preparation and RF conditioning of all power couplers. Details on these topics can be found in [2] and [7].

This power coupler has been designed to provide 10 kW CW (nominal power for an accelerating field of 6.5 MV/m) and be assembled of both cryomodule and cavity types. All couplers must handle 100% reflected power at maximum forward power.

Production of 30 power couplers has started in September 2008. Since then, the first batch of five couplers was delivered and tested at LPSC. RF windows of these couplers were coated differently: two of them were TiN coated with $30 \pm 5\text{ nm}$, one with only $1 \pm 0.2\text{ nm}$ and, finally, two without any coating. All windows were made in the same run.

RF Conditioning

The first window with $30 \pm 5\text{ nm}$ coating broke at 7 kW CW, after only 25 min of normal conditioning process and strong and continuous deterioration of the vacuum pressure at 2 kW CW. As illustrated on Fig. 15, the power coupler showed a “burnt” surface state.

For the second $30 \pm 5\text{ nm}$ coated window conditioning, the power ramp-up timescale was increased (level of 50 s instead of 10 s previously). Additionally, a sensor was set on the external conductor, close to the brazed joint of the window for monitoring. After 85 min, the window broke at 4 kW CW while the window temperature rose up to 120°C (pink curve on Fig. 16). By comparison, one can see on the same Fig. B, the temperature evolution (up to 4

kW CW also) of one of the power couplers with non-coated window (purple curve).



Figure 15: SS-03 power coupler before (left) and after (right) RF conditioning up to 7 kW CW and the break of the window.

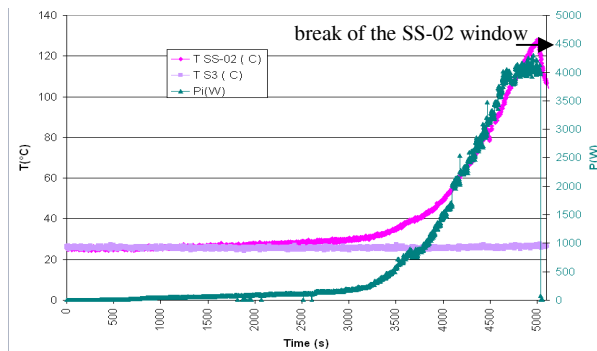


Figure 16: Temperature (°C) and power (W) versus time (s) of n°SS-02 coupler (30 ± 5 nm TiN coated) and n°S3 coupler (non-coated).

Following RF conditioning of remaining couplers were successful. The three couplers (with a TiN coating of 1 ± 0.2 nm and without TiN coating) were conditioned up to 35 kW CW, in travelling wave mode (resp. Fig. 17, 18). One has to note that the coupler with coated window showed an important multipacting activity at low power levels (blue peaks on Fig. 17) together with a warm-up of the external conductor (close to the brazed joint of the window).

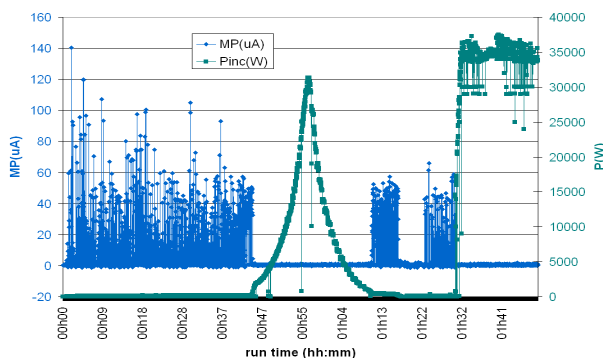


Figure 17: Power (W) level and multipacting activity (µA) versus running time for the 1 ± 0.2 nm TiN coated coupler.

Studies are currently under progress to understand the breaks of the 30 ± 5 nm TiN coated windows. Was the TiN coating thickness too thick? Was there a problem

during the coating process taking into account that the coating was made before the brazing of the window?

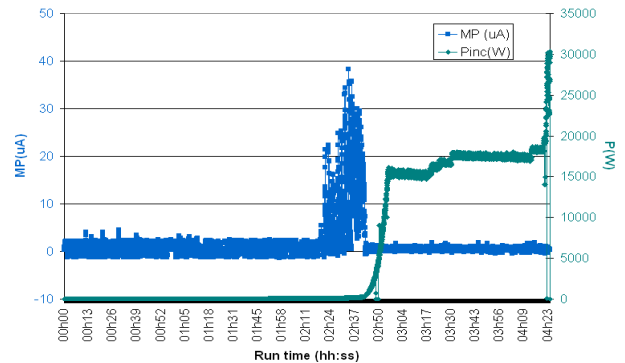


Figure 18: Power (W) and multipacting activity (µA) versus running time for a non-coated coupler.

PRODUCTION STATUS

As a conclusion, TiN coating on coupler window produces an extra thermal load to the superconducting cryomodules and doesn't help for multipacting reduction. For these reasons, we chose not to continue with coated windows for the remaining power couplers production. Production of the twenty five couplers left is now under way. Next delivery of five more couplers is expected at the end of October 2009. The goal is to condition the last coupler mid of 2011.

ACKNOWLEDGMENTS

The author would like to thank P. Bosland and Y. Gomez-Martinez for their contribution to this paper.

The work done at IPN Orsay is supported, via the SUPRAtech platform, by the General Council of Essonne department and the Regional Council of Ile-de-France.

REFERENCES

- [1] Information on the Physics Case of SPIRAL 2: <http://ganinfo.in2p3.fr/research/developments/spiral2>
- [2] Y. Gomez Martinez et al., "Last SPIRAL 2 10kW CW RF Coupler design", LINAC08, Victoria September 2008, THP076, p. 969.
- [3] H. Saugnac et al., "RF and cryogenics tests of the first beta 0.12 SPIRAL2 cryomodule", LINAC08, Victoria, September 2008, THP009, p. 792.
- [4] P-E. Bernaudin et al., "Design of the Low-Beta, Quarter-Wave Resonator and its Cryomodule for the SPIRAL2 Project", EPAC 2004, Lucerne, July 2004.
- [5] P-E. Bernaudin et al., "Tests of the low beta cavities and cryomodules for the SPIRAL2 linac", this conference.
- [6] G. Devanz, "SPIRAL2 Resonators", SRF 2005, Ithaca, July 2005, MoPO2.
- [7] Y. Gómez Martínez et al., "SPIRAL 2 coupler preparation and RF conditioning", SRF 2007, Beijing, October 2007.